

New foreground markers for Drosophila cell segmentation using marker-controlled watershed

Rim Rahali¹, Yassine Ben Salem¹, Noura Dridi², Hassen Dahman^{3,4}

¹MACS Research Laboratory-LR16ES22, National Engineering School of Gabes, Gabes University, Gabes, Tunisia

²ResCoMath Research Laboratory, National Engineering School of Gabes, Gabes University, Gabes, Tunisia

³LaPhyMNE Research Laboratory-LR05ES14, Faculty of Sciences of Gabes, Gabes University, Gabes, Tunisia

⁴Department of Electrical Engineering, National Engineering School of Gabes, Gabes University, Gabes, Tunisia

Article Info

Article history:

Received Jul 19, 2021

Revised May 30, 2022

Accepted Jun 14, 2022

Keywords:

Drosophila cells

Fiji software

Foreground markers

Marker controlled watershed

Obj.MPP framework

Segmentation

ABSTRACT

Image segmentation consists of partitioning the image into different objects of interest. For a biological image, the segmentation step is important to understand the biological process. However, it is a challenging task due to the presence of different dimensions for cells, intensity inhomogeneity, and clustered cells. The marker-controlled watershed (MCW) is proposed for segmentation, outperforming the classical watershed. Besides, the choice of markers for this algorithm is important and impacts the results. For this work, two foreground markers are proposed: kernels, constructed with the software Fiji and Obj.MPP markers, constructed with the framework Obj.MPP. The new proposed algorithms are compared to the basic MCW. Furthermore, we prove that Obj.MPP markers are better than kernels. Indeed, the Obj.MPP framework takes into account cell properties such as shape, radiometry, and local contrast. Segmentation results, using new markers and illustrated on real Drosophila dataset, confirm the good performance quality in terms of quantitative and qualitative evaluation.

This is an open access article under the [CC BY-SA](https://creativecommons.org/licenses/by-sa/4.0/) license.



Corresponding Author:

Rim Rahali

Department of Electrical Engineering, National Engineering School of Gabes, Gabes University

Omar Ibn Khattab Road-6029, Tunisia

Email: rim.rahali@enig.rnu.tn

1. INTRODUCTION

The segmentation of biological images is an important step to analyze biological mechanisms. For example, the study of the density and the repartition of cytoplasmic ribonucleoprotein (RNP) granules helps in understanding the different cellular processes of Drosophila. In fact, the RNP granules contain the IGF-II mRNA-binding protein (Imp) that influences the growth of the nervous system of Drosophila. Therefore, the segmentation step is used to detect the cytoplasm that contains the RNP granules, to analyze the growth of the nervous system. The presence of clusters and intensity inhomogeneity complicate the segmentation task. Plenty of segmentation approaches have been proposed to segment biological images. Some of the most widely used are: i) the deformable model approaches [1], where the energy minimization is based on internal and external forces that make contours converge to the boundaries of interest and ii) the region growing approaches [2], where regions are growing by connecting neighboring pixels with similar measures. Thresholding belongs to the region growing approaches, the idea is to separate the object and the background according to a selected intensity threshold. In this category, Otsu [3] and Kapur *et al.* [4] algorithms are widely used, however both suffer from high computational cost. Therefore, they are combined with optimization algorithms. Erwin *et al.* [5] proposed an improved harmony search algorithm (IHSA) with the Otsu algorithm to improve its efficiency. Recently, the deep learning techniques are largely exploited for

image segmentation with variety of applications such as medical [6] and biological ones [7]. For example, in [8] an interesting application for glioblastomas brain tumor segmentation is proposed. The framework consists on segmenting the tumor cells using simple linear iterative clustering algorithm, then classify the brain image as healthy or pathological by applying the convolutional neural networks (CNN). The watershed [9], is a region growing approach, comes from the field of mathematical morphology. It is largely used in image segmentation for different applications. The watershed finds the crest lines in the image gradient using the flooding process [10]. The image gradient is considered as topographic surface, immersed in the water. Each time, the height of the water meets the height of a label, we obtain a new basin with color of the label. The fusion of two basins of different colors is prevented by creating a line. This line presents the watershed. Grau *et al.* in [11] used the watershed to segment gray and white matter from magnetic resonance (MR) images. Besides, it was applied to segment cancer [12] and nuclei in DNA channel for high throughput ribonucleic acid interference (RNAi) fluorescent cellular images [13]. However, the watershed leads either to oversegmentation caused by the background noise or to under segmentation caused by regions with low contrast. Besides, the segmentation depends on the estimation quality of the gradient. To overcome these issues, the marker controlled watershed (MCW) [14] was proposed. The algorithm shows more effectiveness and practicability. The MCW uses predefined markers that represent objects of interest, it starts from these markers. The detected contours divide only the marked regions. The performance of the segmentation depends on the choice of foreground markers. In [15], we have applied the basic algorithm of MCW that uses opening-by-reconstruction and closing-by-reconstruction as foreground markers. These operations are related to the morphology of features in the image which helps in the construction of markers [16]. However, the basic MCW leads to poor performance because foreground markers did not take into account the cell properties within the image. Besides, the opening and closing by reconstruction sometimes reconstructs undesirable regions.

In this paper, we focus on the segmentation of *Drosophila* cells. The latter is particularly difficult due to: i) presence of nonhomogeneous intensities, ii) cell dimensions are different (big, small...), and iii) clustered cells with weak boundaries. In this work, two foreground markers are designed to segment *Drosophila* cells which are: cell kernels, constructed with the software Fiji [17] and Obj.MPP markers, constructed with the software Obj.MPP [18]. Based on these markers, new algorithms are proposed and compared to the basic MCW. Results, evaluated on *Drosophila* cells, confirm the good segmentation performance, evaluated with the Dice and F1 score [19], [20]. Furthermore, the use of foreground markers constructed with Obj.MPP gives better segmentation results compared to kernels. Contours are more refined and desired object are clearly segmented. The paper may be summarized. Section 2 presents MCW for *Drosophila* cell segmentation. Simulation results on *Drosophila* cells are presented and discussed in section 3. We draw our conclusion in section 4.

2. PROPOSED METHOD: MCW FOR DROSOPHILA CELL SEGMENTATION

2.1. Method description

The MCW segments the image, based on predefined markers. The flooding considers the predefined markers rather than all minima of watershed. For segmentation, it is important to use relevant foreground markers to avoid erroneously detected contours and poor results. As described in [11], the MCW algorithm follows five basic steps:

- Step 1: Compute the segmentation function, where dark region represent object to segment. In this paper, the image gradient is considered as the segmentation function. The Sobel operator [21] is calculated to obtain the gradient.
- Step 2: Compute foreground markers which represent a set of connected pixels within each object.
- Step 3: Compute background markers. Pixels that do not belong to any object present the Background. A thresholding operation is used to mark the background. The watershed is performed on the distance transform of the thresholding result. Then, the obtained watershed ridge lines are used as background.
- Step 4: Adjust the segmentation function so that the gradient magnitude image has local minima at constructed new markers.
- Step 5: Compute the watershed of the modified segmentation function.

Here, three algorithms are compared. Steps 1, 3, 4, and 5 are the same for the three algorithms, while the difference is in the step 2 where three foreground markers are presented. The algorithms are detailed.

2.2. Basic MCW

For the basic MCW, foreground markers are constructed using opening-by-reconstruction and closing-by-reconstruction [22]. Opening and closing by reconstruction are an erosion and dilation followed

by a morphological reconstruction. Following the opening with a closing can remove the dark spots and stem marks. Besides, these operations lead to flat maxima in objects, located using `imregionalmax` (for the MATLAB software). Reconstruction based opening and closing are found effective at eliminating small imperfections. In some cases, markers go straight up to the object boundaries. To shrink them, a closing followed by erosion is applied. The algorithm is applied for medical image segmentation [10], [23]. Although, the performance is improved with regards to the classical watershed in particular when dealing with the oversegmentation, the algorithm fails with *Drosophila* images where the number of objects is high, cell dimensions are different (small, big, ...) in addition to the presence of clustered cells.

2.3. MCW Fiji

For the MCW Fiji, kernels are used as foreground markers. These central parts cover all cells to segment within the image. The Fiji software [24] is used to extract kernels from biological images. It is a public software, dedicated to biological image analysis. Since the extracted kernels are very small, we add a dilation step which prevents also kernels to be too far from cell edges.

2.4. MCW Obj.MPP

For the MCW Obj.MPP, the marked point process (MPP) [25] is presented. The MPP was largely used for image segmentation and it is particularly relevant for biological image segmentation [26]. The algorithm successfully addresses issues related to biological images such as the sensitivity to the noise, the shape variability and the background heterogeneity. For the MPP implementation, the Obj.MPP framework [18] developed by Dr. Eric Debreuve was used. The framework provides a whole segmentation algorithm, besides, here the idea is to consider Obj.MPP results as foreground markers, then the previous described steps (section 2.1) are applied. The framework fixes sets of shapes on the image plane and selects the ones best suited with the predefined characteristics provided by the biologist [27]. To compute the framework, a number of parameters is defined such as: i) the value of the quality function, ii) the number of iterations, and iii) the number of birth cells per iteration. These parameters are fixed empirically by considering a panel of choice, and retaining the set of parameters providing better segmentation performance.

2.5. Data description

The three compared algorithms are applied to segment *Drosophila* cells. These images are the most challenging ones in the dataset. They are produced in the context of an RNAi screen at a high throughput confocal microscope Opera (Perkin Elmer) and a 63X water objective. One image contains 686×518 pixels. Furthermore, the dataset is provided by the biologist Dr. Fabienne De Grave as well as their corresponding kernels. These images are difficult to segment due to the presence of inhomogeneous values of intensities and clustered cells. They are named *Drosophila j*, with *j* varying from 1 to 5. The same for the kernel data noted Kernel *j*, with *j* varying from 1 to 5. Object markers (foreground markers), constructed with the Obj.MPP framework, are enumerated as Obj.MPP *j*, with *j* varying from 1 to 5. A normalization step is included to uniformize intensities [28].

3. RESULTS AND DISCUSSION

This section includes qualitative and quantitative evaluation of the three version of the MCW. For the quantitative evaluation, the Dice coefficient is used [19]. It measures the similarity between two different regions. In addition, the F1 score is measured [20]. The given F1 score is a mean calculated over all the F1 score obtained for labelled objects in the image. The n [29], developed by Dr. Eric Debreuve is used to obtain F1 score values. The ground truth is given by Dr. Fabienne De Graeve. Obj.MPP parameters for *Drosophila* dataset are set: the minimum value of the quality is equal to 0.5, the number of iterations is equal to 8,000 and the number of births cells per iteration is equal to 100. In the following, first the oversegmentation results obtained with the watershed algorithm is illustrated, second the three versions of the MCW: the basic MCW, the MCW Fiji, and the MCW Obj.MPP are compared. Performance is attested for noiseless and noisy images.

3.1. Watershed segmentation results

Watershed segmentation results, obtained for *Drosophila 2* are obtained in Figure 1. Figure 1(a) represents the normalized *Drosophila* image. The image gradient is given in Figure 1(b). Finally, Figure 1(c) corresponds to the segmentation result using the watershed algorithm. As observed, *Drosophila 2* is oversegmented using the watershed algorithm. The information provided by Figure 1(c) is not informative and not useful for biologists. To overcome the watershed limit, another algorithm is proposed in the next section.

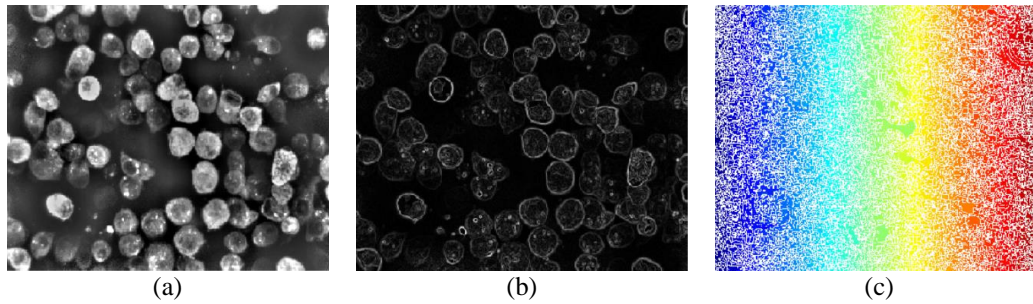


Figure 1. Watershed segmentation result for Drosophila 2 (a) normalized image, (b) image gradient, and (c) watershed result

3.2. Segmentation results using basic MCW, MCW Fiji and MCW Obj.MPP

In this section, qualitative and quantitative evaluations are presented. Moreover, the Otsu algorithm [3] is used for comparison as a reference method for image segmentation. The Otsu thresholding is largely used in literature for biological and medical image segmentation.

3.2.1. Qualitative evaluation

First, the basic MCW and the MCW Fiji are applied to segment Drosophila cells, results are presented in Figure 2. Figure 2(a) shows the normalized image, segmentation result using the basic MCW is illustrated in Figure 2(b). The kernels, used as foreground markers, are given in Figure 2(c). The segmentation result using these kernels is presented in Figure 2(d).

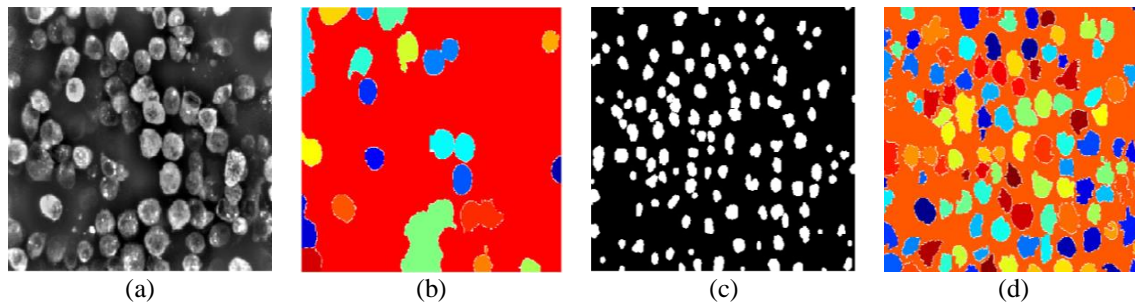


Figure 2. Segmentation results for Drosophila 2 (a) normalized image, (b) result using basic MCW, (c) kernels 2, and (d) result using MCW Fiji

Figure 2(b) illustrates the weak performance of segmentation given by the basic MCW. In fact, a number of cells are detected as background, furthermore; the algorithm cannot handle the case of clusters. On the other hand, with the MCW Fiji, almost all cells are detected as shown in Figure 2(d). This is due to the use of kernels as markers which represent pertinent details. Besides, the MCW Fiji correctly separates the clusters, since each cell in the cluster is defined by its own kernel. Second, segmentation results using the MCW Obj.MPP are illustrated in Figure 3 for Drosophila 2. Figure 3(a) presents the normalized image. Obj.MPP markers are illustrated in Figure 3(b). The segmentation result is given in Figure 3(c), and Figure 3(d) corresponds to the ground truth.

Observations confirm that the MCW Obj.MPP properly segments the Drosophila cells and separates the clustered ones. The segmented image is comparable to the ground truth in terms of cell shapes and dimensions which notably simplify the interpretation and the use of results by the biologists. In Figure 4, comparison between the three algorithms is proposed for Drosophila 2. Figure 4(a) represents the normalized image, the segmentation results using the basic MCW and the MCW Fiji are given in Figure 4(b) and Figure 4(c). As shown in Figure 4(d), the MCW Obj.MPP outperforms the two others algorithms, the contours are better refined and cells boundaries are clearly determined. These results are expected since the Obj.MPP markers are based on prior information about cells as shape, dimension, and radiometry. Therefore, the segmentation is more accurate and focused on target cells.

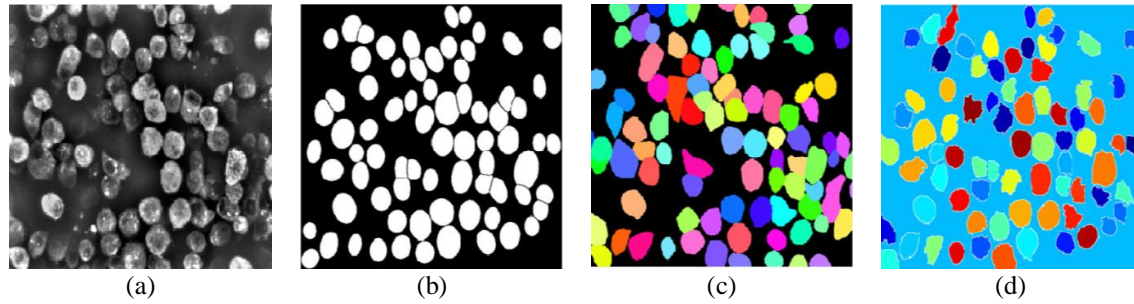


Figure 3. MCW Obj.MPP for Drosophila 2 (a) normalized image, (b) Obj.MMP 2, (c) segmentation result, and (d) ground truth

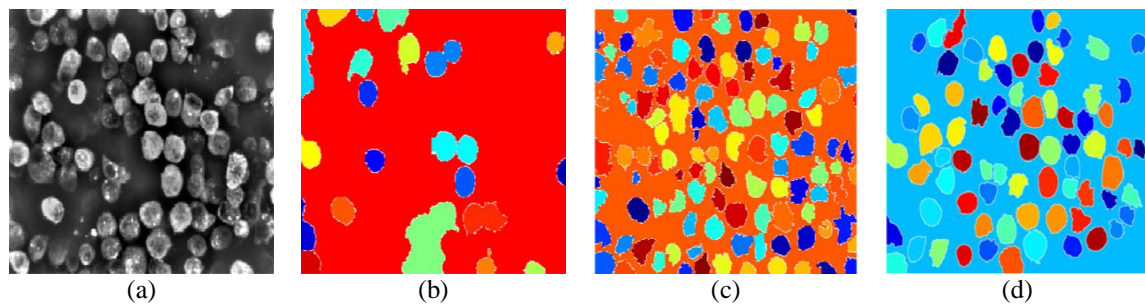


Figure 4. Comparison of segmentation results for Drosophila 2 (a) normalized image, (b) result using basic MCW, (c) result using MCW Fiji, and (d) result using MCW Obj.MPP

3.2.2. Quantitative evaluation

For the numerical evaluation, the Dice coefficient is calculated in Table 1. Over the five images, the mean of the Dice coefficient exceeds 72% for the MCW Obj.MPP while it is only 64% for the MCW Fiji, 63% for the Otsu algorithm, and 49% for the basic MCW. These results attest the superiority of the MCW Obj.MPP, where the Dice similarity is high. The algorithm provides clear segmentation of the cells with different sizes and forms.

Table 1. Dice and mean of F1 score for Drosophila images compared for basic MCW, MCW Fiji, MCW Obj.MPP and Otsu algorithm

		Otsu algorithm	Basic MCW	MCW Fiji	MCW Obj.MPP
Drosophila1	Dice	0.7070	0.5705	0.6501	0.7008
	F1 score	0.4159	0.3564	0.6136	0.7721
Drosophila2	Dice	0.6311	0.4335	0.6819	0.7503
	F1 score	0.3071	0.3539	0.6666	0.8143
Drosophila3	Dice	0.6862	0.6730	0.6975	0.7218
	F1 score	0.3613	0.4424	0.7362	0.7894
Drosophila4	Dice	0.6267	0.4533	0.6422	0.7265
	F1 score	0.2767	0.2471	0.6947	0.8111
Drosophila5	Dice	0.4888	0.3352	0.5321	0.7040
	F1 score	0.0520	0.3380	0.6250	0.8041

While the Dice coefficient measures the similarity between two different regions, the F1 score measures good detections. Again, as illustrated in Table 1, the MCW Obj.MPP outperforms the three other algorithms with a F1 score larger than 77% for all the images and a mean of 80% over the five images. This mean equals to 67% for the MCW Fiji, 35% for the basic MCW, and only 28% for the Otsu algorithm. For the latter, the poor performance is due to the global considering of the threshold that divides the image into background and objects without considering the intensity variations between regions. Moreover, the foreground markers constructed with Fiji and Obj.MPP considerably improve the performance compared to the morphological techniques. Besides, since the Obj.MPP markers consider more details about cell properties than the kernels, especially in terms of shapes and radiometry, the segmentation accuracy is clearly

ameliorated, especially in terms of the smoothness of the detected contours, as observed in the qualitative evaluation (section 3.2.1).

We conclude that the MCW Obj.MPP is more appropriate for *Drosophila* image segmentation. Moreover, the robustness of the MCW Obj.MPP is evaluated in noisy conditions, with adding Gaussian noise to the image. The Dice coefficient and the F1 score are calculated for: 15 dB and 30 dB, as illustrated in Table 2. 10 different noise realizations are considered and the given Dice and F1 score are the mean over these realizations. The mean of F1 score, over the five images, equals 80% for 15 dB and 30 dB. On the other hand, the Dice equals 71% for 30 dB and 70% for 15 dB. Performances are not degraded compared to the noiseless images. The pertinent choice of markers allows a net discrimination between cells and the noise. These results point out the robustness of the MCW Obj.MPP with regards to the noise, and confirm the overall efficiency of the algorithm.

Table 2. Mean of F1 score and Dice for noisy *Drosophila* images using MCW Obj.MPP. Measures are calculated for SNR: 15 dB and 30 dB

	DICE		F1 score	
	30 dB	15 dB	30 dB	15 dB
Drosophila1	0.6951	0.6999	0.7734	0.7835
Drosophila2	0.7460	0.7280	0.8191	0.8239
Drosophila3	0.7113	0.7000	0.7947	0.8013
Drosophila4	0.7226	0.7134	0.8111	0.8111
Drosophila5	0.7028	0.6615	0.8020	0.8041

4. CONCLUSION

For the MCW, the foreground marker choice has a great impact on the segmentation result, especially for biological images. In this paper, two new foreground markers are proposed: kernels, and Obj.MPP markers. They are constructed respectively with the Fiji and the Obj.MPP software's, based on cell properties such as shape and radiometry. Qualitative and quantitative evaluations on real noisy and noiseless images of *Drosophila* are performed using three proposed algorithms: the basic MCW, the MCW Fiji, and the MCW Obj.MPP. Using the MCW Fiji improves results compared to the basic MCW where markers are obtained using morphological techniques. Besides, the MCW Obj.MPP outperforms the MCW Fiji and the basic MCW. The MCW Obj.MPP deals with the intensity inhomogeneity within *Drosophila* images as well as the presence of clustered cells where the basic MCW fails. Furthermore, the contours obtained with the Obj.MPP markers are more refined compared to the ones provided by the Fiji software. The more cell specificities are taken into account, the more the segmentation accuracy is improved. For future work, we aim to increase the precision of the segmentation result using a postprocessing step. The operations performed at the postprocessing can be morphological operations such as the objection elimination on the border edge or the elimination of unusual objects. Finally, the application can be extended to larger dataset and other fields such as medical one.

ACKNOWLEDGEMENTS

The authors would like to thank Dr. Fabienne De Graeve who helped the first author and provided him with the data source. We would thank Professor Xavier Descombes for hosting the first author at the Computer Science, Signals and Systems Laboratory (I3S), Morpheme team, INRIA Sophia Antipolis, France.





REFERENCES

- [1] N. S. M. Noor, N. M. Saad, A. R. Abdullah, and N. M. Ali, "Automated segmentation and classification technique for brain stroke," *International Journal of Electrical and Computer Engineering (IJECE)*, vol. 9, no. 3, pp. 1832–1841, Jun. 2019, doi: 10.11591/ijece.v9i3.pp1832-1841.
- [2] M. Rmili, A. El Moutaouakkil, M. M. Saleck, M. Bouchaib, F. Adnani, and E. M. El Aroussi, "A new approach to the detection of mammogram boundary," *International Journal of Electrical and Computer Engineering (IJECE)*, vol. 8, no. 5, pp. 3587–3593, Oct. 2018, doi: 10.11591/ijece.v8i5.pp3587-3593.
- [3] N. Otsu, "A threshold selection method from gray-level histograms," *IEEE Transactions on Systems, Man, and Cybernetics*, vol. 9, no. 1, pp. 62–66, Jan. 1979, doi: 10.1109/TSMC.1979.4310076.
- [4] J. N. Kapur, P. K. Sahoo, and A. K. C. Wong, "A new method for gray-level picture thresholding using the entropy of the histogram," *Computer Vision, Graphics, and Image Processing*, vol. 29, no. 3, pp. 273–285, Mar. 1985, doi: 10.1016/0734-189X(85)90125-2.
- [5] E. Erwin, S. Saparudin, and W. Saputri, "Hybrid multilevel thresholding and improved harmony search algorithm for segmentation," *International Journal of Electrical and Computer Engineering (IJECE)*, vol. 8, no. 6, pp. 4593–4602, Dec. 2018, doi: 10.11591/ijece.v8i6.pp4593-4602.





- [6] M. H. Hesamian, W. Jia, X. He, and P. Kennedy, "Deep learning techniques for medical image segmentation: achievements and challenges," *Journal of Digital Imaging*, vol. 32, no. 4, pp. 582–596, Aug. 2019, doi: 10.1007/s10278-019-00227-x.
- [7] J. Funke *et al.*, "Large scale image segmentation with structured loss based deep learning for connectome reconstruction," *IEEE Transactions on Pattern Analysis and Machine Intelligence*, vol. 41, no. 7, pp. 1669–1680, Jul. 2019, doi: 10.1109/TPAMI.2018.2835450.
- [8] M. R. Al-Hadidi, B. AlSaaidah, and M. Al-Gawagzeh, "Glioblastomas brain tumour segmentation based on convolutional neural networks," *International Journal of Electrical and Computer Engineering (IJECE)*, vol. 10, no. 5, pp. 4738–4744, Oct. 2020, doi: 10.11591/ijece.v10i5.pp4738-4744.
- [9] S. Beucher, "Watershed, hierarchical segmentation and waterfall algorithm," in *Computational Imaging and Vision*, Springer Netherlands, 1994, pp. 69–76.
- [10] M. Kaur and G. Jindal, "Medical image segmentation using marker controlled watershed transformation," *International Journal of Computer Science And Technology*, vol. 2, no. 4, pp. 548–551, 2011.
- [11] V. Grau, A. U. J. Mewes, M. Alcaniz, R. Kikinis, and S. K. Warfield, "Improved watershed transform for medical image segmentation using prior information," *IEEE Transactions on Medical Imaging*, vol. 23, no. 4, pp. 447–458, Apr. 2004, doi: 10.1109/TMI.2004.824224.
- [12] X. Chen, X. Zhou, and S. T. C. Wong, "Automated segmentation, classification, and tracking of cancer cell nuclei in time-lapse microscopy," *IEEE Transactions on Biomedical Engineering*, vol. 53, no. 4, pp. 762–766, Apr. 2006, doi: 10.1109/TBME.2006.870201.
- [13] P. Yan, X. Zhou, M. Shah, and S. T. C. Wong, "Automatic segmentation of high-throughput RNAi fluorescent cellular images," *IEEE Transactions on Information Technology in Biomedicine*, vol. 12, no. 1, pp. 109–117, Jan. 2008, doi: 10.1109/TITB.2007.898006.
- [14] M. A. Khan *et al.*, "Brain tumor detection and classification: A framework of marker-based watershed algorithm and multilevel priority features selection," *Microscopy Research and Technique*, vol. 82, no. 6, pp. 909–922, Jun. 2019, doi: 10.1002/jemt.23238.
- [15] R. Rahali, Y. Ben Salem, N. Dridi, and H. Dahman, "Drosophila image segmentation using marker controlled watershed," in *2020 17th International Multi-Conference on Systems, Signals and Devices (SSD)*, Jul. 2020, pp. 191–195, doi: 10.1109/SSD49366.2020.9364176.
- [16] I. Terol-Villalobos and D. Vargas, "A study of openings and closings with reconstruction criteria," *Mathematical morphology*, CSIRO, Melbourne, Australia, pp. 413–423, 2008.
- [17] E. T. Arena, C. T. Rueden, M. C. Hiner, S. Wang, M. Yuan, and K. W. Eliceiri, "Quantitating the cell: turning images into numbers with ImageJ," *WIREs Developmental Biology*, vol. 6, no. 2, Mar. 2017, doi: 10.1002/wdev.260.
- [18] E. Debreuve, "Obj.MPP." Accessed: Jan. 10, 2021. [Online]. Available: <https://gitlab.inria.fr/edebreuv/Obj.MPP>
- [19] A. Mansoor *et al.*, "Segmentation and image analysis of abnormal lungs at CT: current approaches, challenges, and future trends," *RadioGraphics*, vol. 35, no. 4, pp. 1056–1076, Jul. 2015, doi: 10.1148/rg.2015140232.
- [20] J. Selinummi *et al.*, "Bright field microscopy as an alternative to whole cell fluorescence in automated analysis of macrophage images," *PLoS ONE*, vol. 4, no. 10, Oct. 2009, doi: 10.1371/journal.pone.0007497.
- [21] G. Chaple and R. D. Daruwala, "Design of Sobel operator based image edge detection algorithm on FPGA," in *2014 International Conference on Communication and Signal Processing*, Apr. 2014, pp. 788–792, doi: 10.1109/ICCSP.2014.6949951.
- [22] "Marker-controlled watershed segmentation," *Mathworks*. Accessed: Feb. 01, 2020. [Online]. Available: <https://mathworks.com/help/images/marker-controlled-watershed-segmentation.html>.
- [23] Y. M. Y. Abdallah, M. A. Alkhir, and A. S. Algaddal, "Improvement of brain tumors detection using markers and boundaries transform," *International Journal of Science and Research (IJSR)*, vol. 4, no. 1, pp. 2372–2376, 2013.
- [24] J. Schindelin *et al.*, "Fiji: an open-source platform for biological-image analysis," *Nature Methods*, vol. 9, no. 7, pp. 676–682, Jul. 2012, doi: 10.1038/nmeth.2019.
- [25] X. Descombes, Ed., *Stochastic geometry for image analysis*. Hoboken, NJ, USA: John Wiley and Sons, Inc., 2013.
- [26] X. Descombes, "Multiple objects detection in biological images using a marked point process framework," *Methods*, vol. 115, pp. 2–8, Feb. 2017, doi: 10.1016/j.ymeth.2016.09.009.
- [27] F. De Graeve *et al.*, "Detecting and quantifying stress granules in tissues of multicellular organisms with the Obj.MPP analysis tool," *Traffic*, Aug. 2019, doi: 10.1111/tra.12678.
- [28] A. Furnari, G. M. Farinella, A. R. Bruna, and S. Battiato, "Distortion adaptive Sobel filters for the gradient estimation of wide angle images," *Journal of Visual Communication and Image Representation*, vol. 46, pp. 165–175, Jul. 2017, doi: 10.1016/j.jvcir.2017.03.019.
- [29] E. Debreuve, "Daccuracy." Accessed: Apr. 15, 2020. [Online]. Available: <https://gitlab.inria.fr/edebreuv/daccuracy>.

BIOGRAPHIES OF AUTHORS







Rim Rahali     is a Ph.D. student at the Research Laboratory Modeling, Analysis and Control Systems-MACS, with an Electrical Engineering degree from the National Engineering School of Gabes (2017). She obtained the Bachelor Degree in Experimental science from the Pioneer School of Gabes, Tunisia in 2012. Her researches are in the fields of Electrical and Automatic systems, Control, and modeling. Recently, image processing has been tackled: Segmentation, biological images, preprocessing, and postprocessing. She is affiliated with IEEE as a Young Professional member. She can be contacted at email: rim.rahali@enig.rnu.tn.







Yassine Ben Salem     is an associate professor at the National Engineering School of Gabes, University of Gabes (Tunisia) since 2010. He earned his Electrical Engineer degree at the Engineering school of Monastir (1998) and his Master (2004) and Ph.D. (2011) at the engineering school of Sfax. He is a member of the Research Laboratory Modeling, Analysis and Control Systems-MACS. He has directed more than 50 Engineering projects and masters and 3 theses. His research interest includes ICT technologies, Innovation, Energy and Smart Cities, Smart buildings, and AI. (More than 50 publications and conference presentations in these areas). He has over than 12 years of teaching experience in renewable energy. He is also the founder of the Tunisian association of science and research. He has developed, participated in, and coordinated ICT projects in FP6, FP7, and HORIZON 2020. He can be contacted at email: bensalemy73@yahoo.fr.



Noura Dridi     was born in Tunis, Tunisia, in 1984. In 2008, she received the diploma of engineer degree in Statistic and Data Analysis, from the High School of Statistic and Data Analysis of Tunis. She was a Ph.D. student both at Telecom-Sud Paris and at the University of Lille 1, France. In September 2012, she joined the laboratory of Material and System Integration, at the University of Bordeaux, France, as a post-doctoral researcher. From 2013 to 2019, she worked as an assistant professor at the National Engineering School of Gabes in Tunisia. In April 2019, she joined the Lab-STICC laboratory at IMT Atlantic in Brest, France as a postdoctoral researcher. Her research interest lies in the field of signal/image processing, especially the Markov model, Bayesian approach to the inverse problem, dynamical model. She can be contacted at email: nourradridi@gmail.com.



Hassen Dahman     is a Professor at the Electrical Engineering Department, National Engineering School of Gabes (ENIG), and a member of the LaPhyMNE laboratory at the faculty of science, Gabes, Tunisia. He obtained his Master in Electronics from the Fundamental Electronic Institute, his Ph.D in Physics Sciences, from the University of Paris 11 Orsay-France, and his HDR (Hability to Direct Research) from the National Engineering School of Gabes in thin films and nanocomposites for negatronic devices applications. He is a reviewer in some journals as materials science in semiconductor processing, solar energy materials, and solar cells and vacuum. His main research interest is: High absorbent thin films for flexible solar cells, nanomaterials for gas sensors applications: Heterojunction based solar cells, nanocomposites for negatronic devices, and recently: Image segmentation, internet of things, connected objects, and energy harvesting. He can be contacted at email: h_dahman_2000@yahoo.com.